

Modeling the effect of discrete distributions of Platinum particles in the PEM fuel cell catalyst layer

Firat C. Cetinbas, Ajay K. Prasad, and Suresh G. Advani*

Center for Fuel Cell Research Department of Mechanical Engineering, University of Delaware (USA)

*Corresponding author: Newark, DE 19716-3140, USA, advani@udel.edu

Abstract: The catalyst layer (CL) is a critical component of the fuel cell as it is the site of all of the cell's electrochemical reactions. The ability to tailor the CL's microstructure can help to mitigate electrochemical activation losses and greatly reduce the loading of expensive Platinum (Pt) catalyst. In this study, the basic CL structure, consisting of carbon-supported Pt particles (C/Pt) and an ionomer binder, is investigated numerically using COMSOL. The significance of modeling discrete Pt particles on the carbon support is highlighted by comparing the cell performance results to the case in which the Pt is assumed to be distributed uniformly over the carbon support as a thin layer. The results reveal that the discretely-distributed particle approach can capture diffusion losses due to particle interactions. In contrast, the uniform-coverage assumption is unable to capture the effect of Pt loading on the diffusion-limited region of the performance curve. In addition, a parametric study is conducted to investigate the range of influence of the discretely-distributed Pt particles.

Keywords: Catalyst layer model; Microscopic catalyst layer model; Platinum loading; PEM fuel cell model

1. Introduction

Polymer electrolyte membrane (PEM) fuel cells are among the most environmentally-friendly energy conversion devices, especially for the automotive industry. In the past decade, huge research effort has been devoted to investigate PEM fuel cells with numerical and experimental methods. Researchers have primarily focused on the components within PEM fuel cells to find the optimal design and improve performance. Among these components, the catalyst layer (CL) is the most significant as it accommodates all of the cell's electrochemical reactions. In addition, one of the main cost drivers of PEM fuel cells is the amount Pt required to catalyze the electrochemical reactions within the CL. A

better understanding of the processes with the CL can lead to improved fuel cell performance and reduce the amount of Pt required.

For the success of any numerical study, it is important to construct a realistic model of the CL with an accurate representation of its microstructure. Several approaches have been reported in the literature for this purpose. Most of them focused on macroscale CL models that can be applied at the cell level to investigate the entire transport process within the fuel cell. These macroscale models generally represent the CL as a homogeneous structure and can be classified as interface models [1], homogeneous models [2], thin film models [3], and agglomerate models [4]. Among these macroscale models, the agglomerate model provides the most comprehensive description of the CL.

Other studies focus directly on the CL microstructure and are called microscale models. For instance, the studies of Bultel et al. [5-8] considered the CL as a set of discrete catalyst nanoparticles. In a similar manner, Yan et al. [9] considered the discrete configuration of Pt particles and proposed a microscopic model to investigate a single catalyst particle consisting of carbon-supported Pt nanoparticles with an ionomer binder. They investigated the effect of Pt particle properties on the performance curves. However, investigating a single catalyst particle by itself cannot identify the optimal composition of the entire CL. In order to optimize the entire CL structure one needs to consider the interactions between the catalyst particles, ionomer binder, and the pores as in the studies of Lange et al. [10, 11] whose model investigates the CL at the pore scale. They reconstructed a CL section consisting of carbon (C) spheres covered by a uniform layer of Pt, with the ionomer film coating the Pt-covered C spheres and the gas pores between the C spheres. They investigated the effective properties of the CL (such as effective diffusivity and conductivity) using this numerically-generated CL architecture.

The microscopic models may provide a better understanding of the influence of Pt particle size and distribution on fuel cell performance, and allow us to optimize the Pt catalyst loading. In the current study, we have developed a microscopic model by extending ideas from [9, 10, 11]. Yan et al. [9] modeled a single catalyst particle in conjunction with the constitutive relations provided by the agglomerate approach. In contrast, we directly consider the reaction-diffusion phenomena at the single catalyst-particle level based solely on the geometric parameters of the particles (no constitutive relations are used) as in [5-8]. The main goal of our work is to point out the significance of accounting for the Pt particles discretely in pore-scale models such as [10, 11]. In this context, the limitations imposed by the uniform Pt-coverage assumption vis-à-vis the modeling of discrete Pt particles on the carbon support are emphasized.

This paper is organized as follows. We first present the geometric construction of our discrete Pt-particle model, along with the governing equations, and parameters used in the simulation. Next, we present fuel cell performance results from the discrete particle case and compare them with results from the baseline case in which a thin, uniform layer of Pt is assumed to completely cover the C support. We show that the uniform coverage assumption fails to capture the effect of variation in reaction surface area, whereas the discretely-distributed particle approach can indeed capture diffusion losses due to particle interactions. Finally, a parametric study is carried out to understand the effect of Pt particle size with constant volume fraction, number of Pt particles, Pt particle distribution, and ionomer film thickness.

2. Model Description

The complex CL structure can be described as a mixture containing C|Pt, ionomer binder, and gas pores. The transport process in the CL starts with the diffusion of reactant gases into the pores. In the absence of flooding by liquid water, the reactant dissolves in the ionomer and is transported towards the active reaction sites where the three-phase contact (ionomer, Pt and C) is present. Finally, the electrochemical

reactions at the reaction sites generate voltages that drive the electronic and ionic current flows.

This study focuses on the active reaction sites without explicitly accounting for the presence of pores. An ideally-shaped cathode C|Pt particle covered by the ionomer binder is investigated with a 3D numerical model generated in COMSOL 4.3. The goal of this study is to overcome the shortcomings due to the assumption of a uniform Pt-layer coverage on the C particle used by Lange et al. [10, 11]. Therefore, the C|Pt particle domain is modeled both with a uniform Pt layer assumption as in [10, 11], and by accounting for the discrete distribution of Pt particles as in [9]. The computational domains for both cases are illustrated in Fig. 1. For the latter case, the ideally-shaped spherical Pt particles on the C support are generated with a script written in MATLAB which allows control of the particle's size and distribution.

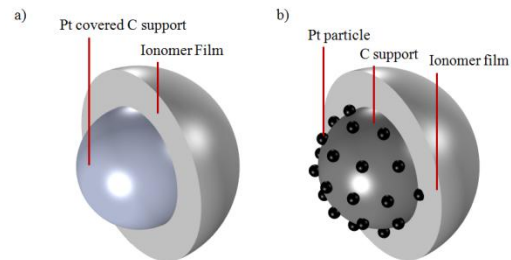


Figure 1. (a) Carbon support uniformly covered with a thin Pt layer; (b) Pt particles modeled discretely on carbon support.

For the C|Pt particles in Fig. 1, the transport phenomena can be reduced to diffusion and reaction of the reactants, and current conduction. For simplicity, the local overpotential is considered constant because the potential drop is expected to be negligible in such a nanoscale domain. Even at the CL level [8], the overpotential varies less than 0.01 %. With the constant overpotential assumption, the current density solely becomes a function of reactant concentration. We also assume isothermal conditions for the CL transport processes. Based on these assumptions, the cathode transport process can be described by the following diffusion equation:

$$\nabla \cdot (D \nabla C_{O_2}) = 0 \quad (1)$$

where D is the diffusivity of O_2 in the ionomer which is calculated from the following equation [12]:

$$D = 3.1 \times 10^{-3} \exp\left(-\frac{2768}{T}\right) [cm^2/s] \quad (2)$$

It is important to note that the electrochemical process is described by the reactions on the surface of the uniformly Pt-covered C sphere, and the surfaces of the discrete Pt particles. In the numerical model, the electrochemistry is interpreted by a boundary condition on the active surfaces that describes the reactant consumption flux as:

$$\dot{N} = \frac{dC_{O_2}}{d\vec{n}} = \frac{i}{4F} \quad (3)$$

where the generated current density (i) is given by the Butler-Volmer equation as:

$$i = i_0 \left[\frac{C_{O_2}}{C_{O_{2,s}}} \exp\left(-\frac{\alpha_c F}{RT} \eta\right) - \exp\left(\frac{(1 - \alpha_c) F}{RT} \eta\right) \right] \quad (4)$$

where i_0 is the exchange current density, $C_{O_{2,s}}$ is the O_2 concentration at the outer wall of ionomer film, η is the constant local overpotential, and α_c is the cathodic charge transfer coefficient. $C_{O_{2,s}}$ is defined as a Dirichlet boundary condition at the outer surface of the ionomer film. Assuming a constant operating pressure P_{O_2} , the reactant surface concentration can be calculated using Henry's constant H [12] as:

$$C_{O_{2,s}} = \frac{P_{O_2}}{H} \quad (5)$$

The current density is calculated based on the approach presented in [12] as:

$$I = FD \left(\vec{n}_x \frac{dC_{O_2}}{dx} + \vec{n}_y \frac{dC_{O_2}}{dy} + \vec{n}_z \frac{dC_{O_2}}{dz} \right)_{@r=r_C+\delta} \quad (6)$$

where r_C is the radius of the C sphere, and δ is the thickness of the ionomer film. The

parameters and operating conditions utilized in the simulations are listed in Table 1.

Table 1. Parameters used for simulating the base case

Temperature	T	353.15[K]
Oxygen pressure	P_{O_2}	1.5 [atm]
Henry's constant	H	0.3125 [atmm ³ /mol]
Pt radius	r_{Pt}	2 [nm]
C radius	r_C	20 [nm]
Ionomer film thickness	δ	12 [nm]
Charge transfer constant	α_c	0.5
Exchange current density	i_0	6e-8[A/cm ²]

The diffusion equation coupled with a nonlinear flux term at the active boundaries is solved with COMSOL 4.3 by using a stationary parametric solver. A sweep study is conducted in order to plot the performance curves. It is important to note that the high reaction rates on the active boundaries can cause the solver to return negative concentration values which are not physical; this problem can be solved by increasing the mesh density near the active boundaries. Another way is to apply a logarithmic transformation to the governing equation in order to ensure stability of the diffusion equation.

3. Results

In this study, we compare results for the C|Pt particle models presented by Yan et al. [9], and Lange et al. [10, 11]. Yan et al. [9] accounted for discrete Pt particles on a C support whereas Lange et al. [10, 11] assumed that the C support is uniformly covered by a thin Pt layer as shown in Fig. 1. The performance curves from these two approaches are presented in Fig. 2. It is important to note that the surface area of the uniform Pt layer is equal to the total active area of the Pt particles in the discrete particle case.

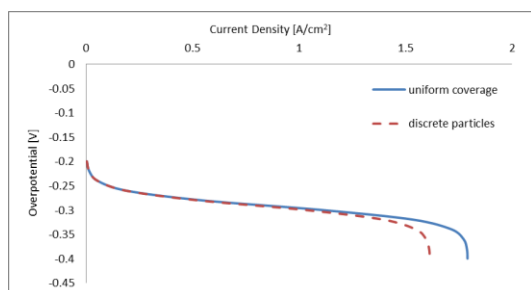


Figure 2. Comparison of performance obtained with the uniform coverage and discrete particle approaches

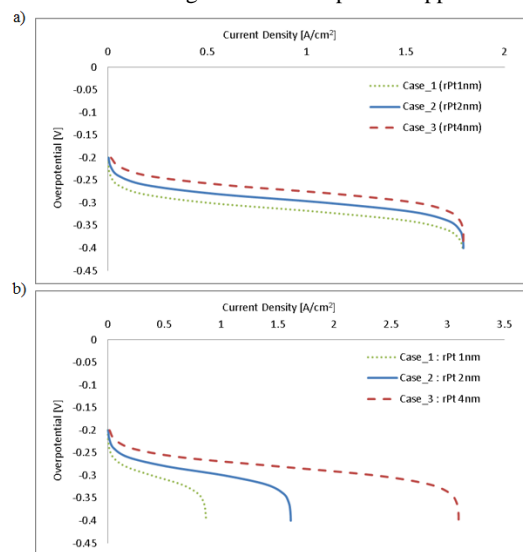


Figure 3. Effect of catalyst loading on performance obtained with (a) the uniform coverage approach, and (b) the discrete particle approach

Figure 2 indicates that the performance plots are in agreement in the activation and ohmic regions at low and intermediate current densities, respectively. However, the discrete particle approach predicts an earlier entry into the diffusion-limited region at high current densities. In other words, the discrete modeling of particles resulted in increased diffusion losses. It may be inferred that the Pt-particle interactions impose an additional diffusion loss whereas the diffusion loss for the uniform Pt-coverage case arises solely from the ionomer film coating the C|Pt particle.

Next, we investigate the variation in the Pt loading which changes the reaction surface area. In order to increase the Pt loading for the discrete particle approach, one can increase the Pt-particle size or the number of particles. Here, we chose to increase the particle size so as to preserve the particle distribution; hence, the total

active surface area varies as the square of Pt-particle radius. For the uniform coverage assumption, we modified the active area by employing a multiplicative factor that is equivalent to increasing Pt utilization.

Figure 3a indicates that for the uniform coverage case, the variation in reaction surface area produces expected changes in the activation region of the polarization plot. However, all three curves indicate the same limiting current in the diffusion-limited region. On the other hand, the discrete particle approach indicates that the performance depends strongly on reaction area in both the activation and diffusion-limited regions as seen in Fig. 3b. Consistent with the results from Fig. 2, comparison between Figs. 3a and 3b suggests that particle interactions are important in the diffusion-limited region, whereas the diffusion losses are dominated by the ionomer film in the uniform coverage case.

This comparison reveals the importance of modeling the Pt as discrete particles. This conclusion leads us to examine the effect of variations in the parameters related to the discrete Pt particles. Therefore, we conducted a parametric study to understand the effect of particle size while maintaining a constant weight ratio between Pt, C, and ionomer; particle number; particle distribution; and ionomer film thickness on fuel cell performance.

Results from experiments have shown that smaller Pt particles with the same CL composition give better performance due to an increase in the reaction surface area. In order to simulate this case, we need to keep the volume fraction of Pt, C, and ionomer constant. Accordingly, we changed the C sphere size and ionomer film thickness with the Pt-particle radius. We could have achieved the same effect by increasing the number of Pt particles for the same weight ratio, but the preferred way is computationally more efficient.

Figure 4 shows the influence of C|Pt particle size on performance. In Fig. 3b we showed that the performance increases with the increasing Pt-particle size due to increased surface area. However, in Fig. 4 we maintained a constant weight and volume fraction while decreasing the Pt-particle size. Figure 4 clearly indicates that performance improves as the catalyst particles become smaller.

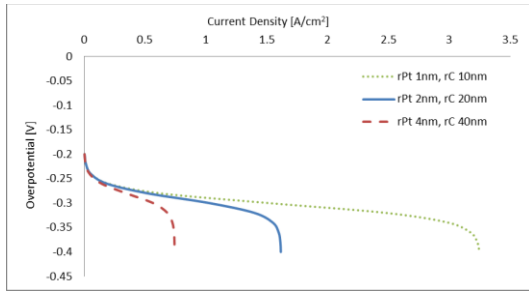


Figure 4. The effect of catalyst particle size on performance using the discrete particle approach

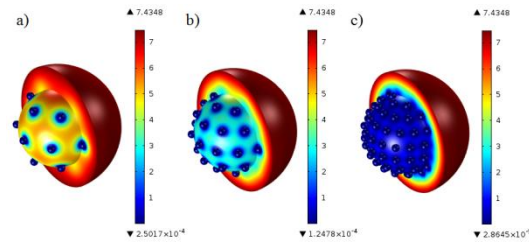


Figure 5. Concentration contours of reactant in mol/m^3 obtained with the discrete particle approach for $\eta = -0.4 \text{ V}$, $r_C = 20 \text{ nm}$, and $r_{Pt} = 2 \text{ nm}$; (a) $NPt = 20$; (b) $NPt = 44$; (c) $NPt = 104$

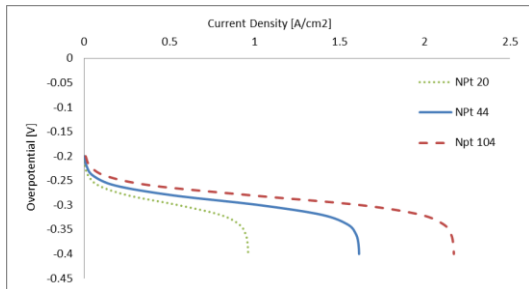


Figure 6. The effect of number of Pt particles on performance obtained with the discrete particle approach

As previously stated the Pt loading can also be increased by increasing the number of particles. The effect of increasing the number of Pt particles on the reaction concentration contours, and the performance plot are illustrated in Figs. 5 and 6, respectively.

Figure 5 shows that the reactant consumption increases with the number of catalyst particles. Reactant consumption grows as surface area increases, and the performance improves for the same reason. As expected, Fig. 6 shows that the best performance is obtained with the highest number of Pt particles.

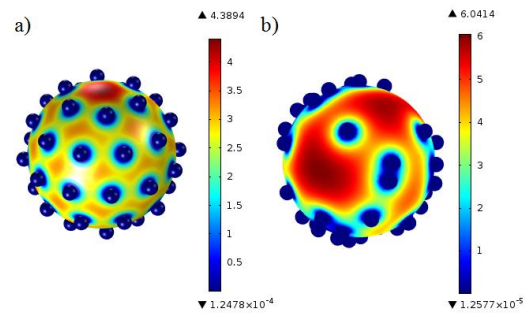


Figure 7. The effect of Pt particle distribution on concentration contours in mol/m^3 obtained with the discrete particle approach for $\eta = -0.4 \text{ V}$, $r_C = 20 \text{ nm}$, and $r_{Pt} = 12 \text{ nm}$; (a) equi-spaced particles; (b) randomly distributed particles

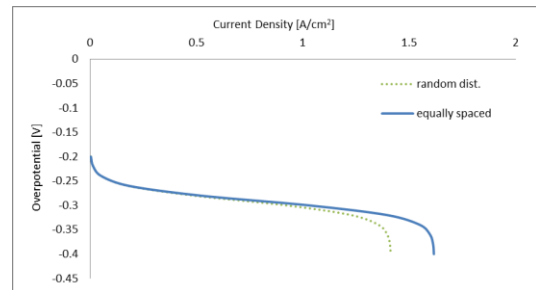


Figure 8. Effect of Pt particle distribution on performance obtained with the discrete particle approach

For all the previously examined cases, the particles are uniformly distributed over the surface of the C sphere. The effect of inter-particle distance and non-uniform particle distribution on performance can be investigated by employing randomly distributed Pt particles. The effect of particle distribution on concentration contours and performance are shown in Figs. 7 and 8, respectively.

Figure 7 illustrates the effect of non-uniform Pt particle distribution on the reactant consumption. It is seen that the minimum concentration obtained with the random distribution is about 10 times lower than the one obtained with the uniform distribution because several particles are very closely clustered in the former case. Similarly, the highest concentration in the random distribution case is higher than the one in the equi-spaced case due to the presence of large dead zones as shown in Fig. 7b. These large dead zones would cause lower overall performance for the random distribution case as verified in Fig. 8.

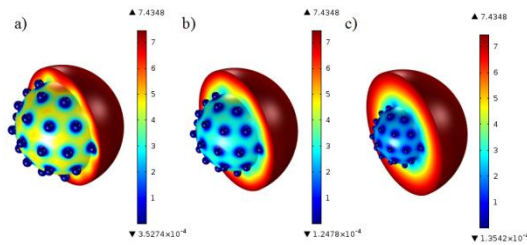


Figure 9. The effect of ionomer film thickness on concentration contours in mol/m^3 obtained with the discrete particle approach for $\eta = -0.4 \text{ V}$, $r_C = 20 \text{ nm}$, and $r_{Pt} = 2 \text{ nm}$; (a) $\delta = 6 \text{ nm}$; (b) $\delta = 12 \text{ nm}$; (c) $\delta = 24 \text{ nm}$

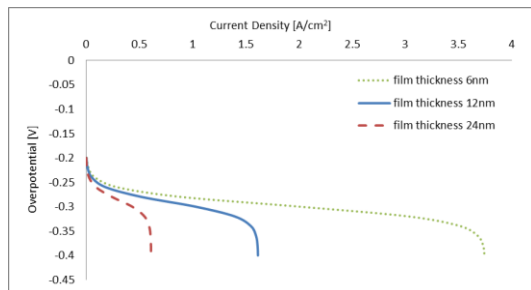


Figure 10. The effect of ionomer film thickness on performance obtained with the discrete particle approach

The influence of ionomer film thickness on the reactant concentration contours and the performance obtained by the discrete particle approach are shown in Figs. 9 and 10, respectively. The concentration contours in Fig. 9 reveal that a thicker ionomer film leads to greater reactant depletion on the C-support surface due to the film's higher diffusion resistance. This result is confirmed by the performance plots in Fig. 10 where a thicker ionomer film forces an earlier entry into the diffusion-limited region, and a smaller limiting current.

4. Summary and Conclusions

This study focused on the numerical investigation of the catalyst layer in a PEM fuel cell. Specifically, we studied a single C|Pt particle surrounded by an ionomer film. A spherical C|Pt particle is considered under two assumptions: (i) a uniform coverage case in which a thin layer of Pt catalyst uniformly covers the carbon support, and (ii) discrete Pt particles which are distributed over the surface of the carbon support.

Results from these two cases highlighted the importance of modeling Pt particles discretely. It is revealed that the diffusion losses are properly captured by modeling the catalyst layer with discrete Pt particles, whereas the uniform coverage case shows the same diffusion-limited performance irrespective of Pt loading.

A parametric study was conducted to investigate the effect of different parameters for the discrete particle approach. It was shown that increasing the amount of reaction surface area increases performance. Consistent with the experimental observations, it was also shown that smaller catalyst particles provide better performance. In addition, the distribution of the Pt particles on the carbon support affects the performance: uniformly-distributed particles yielded a higher performance than the case with randomly-distributed particles. Finally, it was confirmed that a thicker ionomer film increases diffusion losses.

5. References

1. T. Berning, D.M. Lu, N. Djilali, J. Power Sources 106 (1–2) (2002) 284-294
2. D. Harvey, J.G. Pharoah, K. Karan, J. Power Sources 179 (2008) 209–219
3. D.M. Bernardi, M.W. Verbrugge, AIChE J. 37 (8) (1991) 1151-1163
4. K. Broka, P. Ekdunge, J. Appl. Electrochem. 27 (3) (1997) 281-289
5. Y. Bultel, P. Ozil, R. Durand, J. Applied Electrochemistry 28 (1998) 269-276
6. Y. Bultel, P. Ozil, R. Durand, J. Applied Electrochemistry 29 (1999) 1025-1033
7. O. Antoine, Y. Bultel, R. Durand and P. Ozil, Electrochim. Acta, 43 (1998) 3681-3691
8. Y. Bultel, P. Ozil, R. Durand, J. Applied Electrochemistry 30 (2000) 1369-1376
9. Q. Yan, J. Wu, Energy Conversion and Management, 49 (2008) 2425-2433
10. K.J. Lange, P.C. Sui, N. Djilali, J. Power Sources 196 (2011) 3195–3203
11. K.J. Lange, P.C. Sui, N. Djilali, J. Power Sources 208 (2012) 354–365
12. R. M. Rao, R. Rengaswamy, J. Power Sources 158 (2006) 110 -123

6. Acknowledgements

This work was funded by the Federal Transit Administration.